Joint Beamforming Design under Target Reflected Interference in RIS-Assisted Bi-Static ISAC System

Mohsin Ali
Department of Electronic Engineering
Hanyang University
Seoul, Republic of Korea
mohsin0987@hanyang.ac.kr

Abdulahi Abiodun Badrudeen
Department of Electronic Engineering
Hanyang Universit
Seoul, Republic of Korea
aabadrudeen@hanyang.ac.kr

Seungwoo Baek
Department of Electronic Engineering
Hanyang Universit
Seoul, Republic of Korea
swbaek@hanyang.ac.kr

Yekaterina Kim
Department of Electronic Engineering
Hanyang Universit
Seoul, Republic of Korea
aabadrudeen@hanyang.ac.kr

Sunwoo Kim
Department of Electronic Engineering
Hanyang University
Seoul, Republic of Korea
remero@hanyang.ac.kr

***Abstract*—Integrated sensing and communication (ISAC) and reconfigurable intelligent surfaces (RIS) are emerging technologies for future 6G wireless communication, aiming to overcome spectrum scarcity and manipulate the wireless propagation environment, respectively. This paper investigates a RIS-assisted bi-static ISAC system designed for the scenario where the line-of-sight (LoS) link between the transmitter, communication user, and target is obstructed. We assume that both the user and target are located close to each other, and there is a possibility that the user will also receive the undesired sensing signal from the target, which affects the user's communication rate. We aim to jointly optimize the transmit beamformer and the RIS reflection coefficients to maximize the user's communication rate while satisfying the minimum sensing signal-to-noise ratio (SNR) requirement, transmit power, and RIS unit-modulus constraints. An efficient alternating optimization (AO) algorithm is developed by leveraging fractional programming (FP), semi-definite relaxation (SDR), and minorization-maximization (MM) techniques to solve this non-convex problem. Simulation results show the advantage of deploying RIS in ISAC in a shadowed environment and the efficacy of our proposed algorithm.**

***Index Terms*—Integrated sensing and communication (ISAC), reconfigurable intelligent surface (RIS), target reflected interference, communication rate, 6G wireless communication.**

I. INTRODUCTION

The increasing demand for Internet of Things (IoT) applications and the rapid growth of smart devices connected to wireless networks have made the wireless spectrum a scarce resource. ISAC has emerged as a key technology in beyond fifth generation (B5G) and sixth generation (6G) with the potential to improve spectrum efficiency [1], [2]. Integrated sensing and communication (ISAC) combines radar sensing and wireless communication functions into a single unified system. Instead of designing separate communication and sensing modules, ISAC utilizes shared hardware, spectrum, and signal processing techniques to execute both functions simultaneously [3]–[5].

Considering the practical wireless communication networks scenarios, obstructions in the LoS links between network elements and other unfavorable propagation conditions seriously degrade the signal transmission efficiency and quality. Recently, reconfigurable intelligent surfaces (RIS) have emerged as a promising and cost-effective solution to overcome this issue and also to increase channel capacity and service coverage [6]. RIS consists of many passive reflecting elements that change the propagation path of electromagnetic waves without needing extra energy. This passive feature of RIS provides several advantages, including lower energy consumption, avoiding complex signal processing, and greater deployment flexibility [7], [8]. Furthermore, RIS can increase the degree of freedom (DoF) of beam design while providing more LoS links to handle complex electromagnetic environments. The potential of RIS to transform harsh wireless propagation environments that are traditionally considered unmanageable into controllable ones opens new ways of reconfiguring the wireless propagation environment with more desirable characteristics [9], [10].

Extensive research is being carried out on the integration of RIS into the ISAC system to leverage the potential of RIS in the form of additional virtual LoS links between the network elements to enhance the network performance. Authors in [11] proposed a comprehensive perspective on the channel modeling for the prospective standardization of unified RIS and ISAC techniques. Joint waveform and RIS phase shifts optimization is proposed in [12] to enhance the signal to interference plus noise ratio (SINR) for sensing and to reduce the multiple user interference (MUI) for communication. A novel successive convex approximation (SCA) based method for joint beamforming design is proposed in [13] to address the security challenges in RIS-enabled ISAC systems. In [14], a simultaneous transmission and reflection reconfigurable intelligent surface (STAR-RIS) aided downlink ISAC system is investigated for simultaneous communication with an indoor user terminal and sensing and tracking of the outdoor dynamic scatterers. To balance multi-target fairness and communication security, the joint beamforming design for a secure RIS-assisted ISAC system is investigated in [15]. A penalty based iterative method is adopted in [16] for joint physical layer security and covert communication while optimizing beamforming for effective sensing and secure data transmission in an active-STAR-RIS assisted ISAC system. To deal with the secure transmission in the ISAC system, the joint design of beamforming, reflection, and receiving filter for the IRS-aided bi-static ISAC system with security constraint is investigated in [17].

In the practical scenarios, the communication user and the target may be located close to each other. Thus, the reflected signal from the target can cause interference to the communication user and can cause degradation in the user's communication rate. However, most of the existing papers did not consider this practical scenario. Therefore, this paper incorporates the target reflected interference into the user's received signal model to investigate the more realistic user's communication rate . We formulate a problem to maximize the user's communication rate by jointly optimizing the transmit beamforming and RIS reflection coefficients while satisfying a minimum sensing signal-to-noise ratio (SNR) requirement, transmit power, and RIS unit-modulus constraints in the given scenario. We propose an alternating optimization (AO) algorithm to iteratively solve this non-convex problem. We use fractional programming (FP) and semi-definite relaxation (SDR) to optimize the active beamforming and minorization-maximization (MM) algorithm for passive beamforming optimization.

II. System Model

Considering the RIS-assisted bi-static ISAC system, which constitutes two ISAC base stations (BS), a RIS, one single antenna communication user, and a single target as shown in Fig. 1. We assume that one ISAC BS acts as a transmitter (Tx) and the other as a receiver (Rx) only [17]. Both the ISAC transmitter and receiver are equipped with $M_t = M_r = M$ uniform linear array (ULA) antennas, where M_t and M_r denote the number of transmit and receive antennas, receptively. RIS contains a uniform planar array (UPA) of N reflecting elements. The LoS links between ISAC Tx to the user and target are disabled due to obstructions between them. Therefore, we contemplate a RIS in the system to create the links between the transmitter, communication user, and target. RIS directs the transmitted signal towards the user and target. We postulate that the user and target are located close enough to each other. Hence, there exists a possibility that the user will also receive the signal reflected by the target. For achieving dual functionality of ISAC i.e., communication and sensing , the transmitter transmits the signal given by

$$\mathbf{x} = \mathbf{w}_c \mathbf{s}_c + \mathbf{w}_s \mathbf{s}_s, \tag{1}$$

where $\mathbf{w}_c \in \mathbb{C}^{M\times 1}$ and $\mathbf{w}_s \in \mathbb{C}^{M\times 1}$ denote the communication and sensing beamforming vectors, respectively, while $\mathbf{s}_c$ and $\mathbf{s}_s$ represent the communication and sensing symbols, respectively.

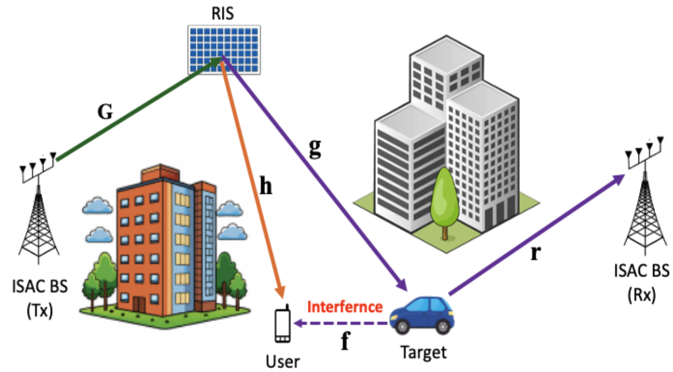

Figure 1. RIS assisted bi-static ISAC system

A. Communication Model

As there is no direct LoS link between ISAC Tx and the user, the transmitted signal reaches at user via RIS. Besides this, user will also receive the reflected sensing signal from the target. Then, the overall signal received by the user can be formulated as

$$y_u = \underbrace{\mathbf{h}^H \mathbf{\Phi} \mathbf{G} \mathbf{x}}_{\text{desired signal}} + \underbrace{\alpha \mathbf{f} \mathbf{g}^H \mathbf{\Phi} \mathbf{G} \mathbf{x}}_{\text{undesired signal}} + n_u, \tag{2}$$

where $\mathbf{G} \in \mathbb{C}^{N\times M}$ represents the channel between ISAC Tx and RIS, $\mathbf{\Phi} = \text{diag}(e^{j\theta_1}, \dots, e^{j\theta_N}) \in \mathbb{C}^{N\times N}$ exhibits the RIS phase shift matrix, $\mathbf{h} \in \mathbb{C}^{N\times 1}$ indicates the channel between RIS and the user, $\mathbf{g} \in \mathbb{C}^{N\times 1}$ denotes RIS to target channel, $\mathbf{f} \in \mathbb{C}^{1\times 1}$ denotes the channel between target and the user, α represents the reflection coefficient of the target, and $n_u \sim \mathcal{CN}(0, \sigma_u^2)$ means additive white Gaussian noise (AWGN) received at the user, having zero mean and variance σ_u^2. The signal to interference plus noise ratio (SINR) at the user can be expressed as

$$\gamma_u = \frac{|\mathbf{h}^H \mathbf{\Phi} \mathbf{G} \mathbf{w}_c|^2 + |\alpha \mathbf{f} \mathbf{g}^H \mathbf{\Phi} \mathbf{G} \mathbf{w}_c|^2}{|\mathbf{h}^H \mathbf{\Phi} \mathbf{G} \mathbf{w}_s|^2 + |\alpha \mathbf{f} \mathbf{g}^H \mathbf{\Phi} \mathbf{G} \mathbf{w}_s|^2 + \sigma_u^2}. \tag{3}$$

B. Sensing Model

There is also no direct LoS link between ISAC Tx and the target. The transmitted signal is directed towards the target with the aid of RIS. ISAC Rx then receives the reflected signal from the target. The reflected sensing signal received at the ISAC Rx can be expressed as

$$y_x = \alpha \mathbf{r} \mathbf{g}^H \mathbf{\Phi} \mathbf{G} \mathbf{x} + n_x, \tag{4}$$

where $\mathbf{r} \in \mathbb{C}^{M\times 1}$ denotes the channel between target and ISAC Rx and $n_x \sim \mathcal{CN}(0, \sigma_x^2)$ represents AWGN received at the ISAC Rx. Then, the sensing SNR of the target received at ISAC Rx is given as

$$\gamma_x = \frac{|\alpha \mathbf{r} \mathbf{g}^H \mathbf{\Phi} \mathbf{G} \mathbf{w_s}|^2}{\sigma_x^2}. \tag{5}$$

III. Problem Formulation and Solution

The main objective of this paper is to maximize the communication rate by jointly optimizing the active beamformer $\mathbf{w}_c$ and $\mathbf{w}_s$ at ISAC Tx and the passive beamforming $\mathbf{\Phi}$ at RIS under the constraints of ensuring sensing performance, the total transmit power of BS, and the unit-modulus constraint of the RIS, which can be described as

$$\begin{aligned}
\text{(P1)}: \max_{\mathbf{w}_c, \mathbf{w}_s, \mathbf{\Phi}} \quad & R_u = \log_2(1+\gamma_u) && \text{(6a)}\\
\text{subject to} \quad & \gamma_x \geq \gamma_{\text{th}}, && \text{(6b)}\\
& \|\mathbf{w}_c\|^2 + \|\mathbf{w}_s\|^2 \leq P_{\text{max}}, && \text{(6c)}\\
& |\phi_m| = 1, \quad \forall m, && \text{(6d)}
\end{aligned}$$

where γ_{th} manifests the predefined sensing SNR threshold and $P_{\max}$ represents the total transmit power. It is noted that the optimization problem in (6a) is non-convex due to quadratic equality constraints and unit modulus constraint on the RIS phase vector ϕ_m. Specifically, the multiplicative coupling of optimization variables $\mathbf{w}_c$, $\mathbf{w}_s$, and $\mathbf{\Phi}$ in the fractional expression of SINR in the objective function and constraints make this problem non-convex in nature and complex to solve directly. Thus, to reduce the complexity of this nonconvex problem, we adopted the AO approach. Firstly, we contemplate the fixed $\mathbf{\Phi}$ to optimize the transmitted beamforming matrix $\mathbf{W}$, then optimize the RIS reflection coefficient matrix $\mathbf{\Phi}$ by considering the fixed $\mathbf{W}$, to maximize the communication rate by meeting the required constraints. We break our optimization problem into two subproblems by exploiting the AO approach as discussed in the next two sub-sections.

A. Active beamformers ($\mathbf{w}_c$, $\mathbf{w}_s$) optimization for fixed $\mathbf{\Phi}$

We define some equivalent channels for simplicity. $\mathbf{h}_{\text{eq}}^H = \mathbf{h}^H\mathbf{\Phi}\mathbf{G}$ and $\mathbf{g}_{\text{eq}}^H = \mathbf{g}^H\mathbf{\Phi}\mathbf{G}$ represent the equivalent channels from the ISAC Tx to the user and target, respectively, with the aid of RIS, while $\mathbf{q}_{\text{eq}}^H = \alpha\mathbf{f}\mathbf{g}_{\text{eq}}^H$ denotes the equivalent channel from the ISAC Tx to the user through RIS and target. Therefore, (3) and (5) can be rewritten as

$$\gamma_u = \frac{|\mathbf{h}_{\text{eq}}^H\mathbf{w}_c|^2 + |\mathbf{q}_{\text{eq}}^H\mathbf{G}\mathbf{w}_c|^2}{|\mathbf{h}_{\text{eq}}^H\mathbf{w}_s|^2 + |\mathbf{q}_{\text{eq}}^H\mathbf{w}_s|^2 + \sigma_u^2}. \tag{7}$$

$$\gamma_x = \frac{|\alpha\mathbf{r}\mathbf{g}_{\text{eq}}^H\mathbf{w_s}|^2}{\sigma_x^2}. \tag{8}$$

We can rewrite the optimization problem (P1) as follow

$$\begin{aligned}
\text{(P2)}: \max_{\mathbf{w}_c, \mathbf{w}_s} \quad & \log_2(1+\gamma_u) && \text{(9a)}\\
\text{subject to} \quad & |\alpha\mathbf{r}\mathbf{g}_{\text{eq}}^H\mathbf{w}_s|^2 \geq \gamma_{\text{th}}\sigma_x^2, && \text{(9b)}\\
& \|\mathbf{w}_c\|^2 + \|\mathbf{w}_s\|^2 \leq P_{\text{max}}. && \text{(9c)}
\end{aligned}$$

Problem (P2) is still non-convex. Therefore, we adopt fractional programming (FP) and semi-definite relaxation (SDR) to explore the solution of the problem. We define some auxiliary variables, $\mathbf{W}_c = \mathbf{w}_c\mathbf{w}_c^H$ and $\mathbf{W}_s = \mathbf{w}_s\mathbf{w}_s^H$. Hence, the user's SINR and SNR at ISAC Rx will be derived as

$$\gamma_u = \frac{\text{Tr}(\mathbf{R}_c\mathbf{W}_c)}{\text{Tr}(\mathbf{R}_c\mathbf{W}_s) + \sigma_u^2}, \tag{10}$$

and

$$\gamma_x = \frac{|\alpha|^2|\mathbf{r}|^2\text{Tr}(\mathbf{g}_{\text{eq}}\mathbf{g}_{\text{eq}}^H\mathbf{W}_s)}{\sigma_x^2}, \tag{11}$$

where $\mathbf{R}_c = \mathbf{h}_{\text{eq}}\mathbf{h}_{\text{eq}}^H + \mathbf{q}_{\text{eq}}\mathbf{q}_{\text{eq}}^H$. The constraint (9b) can be expressed as $\text{Tr}(\mathbf{g}_{\text{eq}}\mathbf{g}_{\text{eq}}^H\mathbf{W}_s) \geq \frac{\gamma_{\text{th}}\sigma_x^2}{|\alpha\mathbf{r}|^2}$. Now, the optimization problem (P2) can be expressed as

$$\begin{aligned}
\text{(P3)}: \max_{\mathbf{W}_c, \mathbf{W}_s} \quad & \log_2\left(1 + \frac{\text{Tr}(\mathbf{R}_c\mathbf{W}_c)}{\text{Tr}(\mathbf{R}_c\mathbf{W}_s) + \sigma_u^2}\right) && \text{(12a)}\\
\text{subject to} \quad & \text{Tr}(\mathbf{g}_{\text{eq}}\mathbf{g}_{\text{eq}}^H\mathbf{W}_s) \geq \Gamma, && \text{(12b)}\\
& \text{Tr}(\mathbf{W}_c + \mathbf{W}_s) \leq P_{\text{max}}, && \text{(12c)}\\
& \mathbf{W}_c,\ \mathbf{W}_s \succeq 0, && \text{(12d)}\\
& \text{rank}(\mathbf{W}_c) = \text{rank}(\mathbf{W}_s) = 1, && \text{(12e)}
\end{aligned}$$

where $\Gamma = \frac{\gamma_{\text{th}}\sigma_x^2}{|\alpha\mathbf{r}|^2}$. This problem still looks harder to solve because of the fractional objective function. To handle the non-convexity of the fractional objective, we employ Dinkelbach's transformation by introducing an auxiliary variable η. The fractional objective function is equivalently rewritten as

$$\max_{\mathbf{W}_c, \mathbf{W}_s} \text{Tr}(\mathbf{R}_c\mathbf{W}_c) - \eta(\text{Tr}(\mathbf{R}_c\mathbf{W}_s) + \sigma_u^2), \tag{13}$$

where η denotes the current estimate of the optimal objective ratio. The problem P(3) cannot be solved directly due to the rank-1 constraints. Therefore, by using the SDR technique and dropping the rank-1 constraints, the resulting convex semidefinite program (SDP) problem can be shown as

$$\begin{aligned}
\text{(P4)}: \max_{\mathbf{W}_c, \mathbf{W}_s} \quad & \text{Tr}(\mathbf{R}_c\mathbf{W}_c) - \eta\big(\text{Tr}(\mathbf{R}_c\mathbf{W}_s) + \sigma_u^2\big) && \text{(14a)}\\
\text{subject to} \quad & \text{Tr}(\mathbf{g}_{\text{eq}}\mathbf{g}_{\text{eq}}^H\mathbf{W}_s) \geq \Gamma, && \text{(14b)}\\
& \text{Tr}(\mathbf{W}_c + \mathbf{W}_s) \leq P_{\text{max}}, && \text{(14c)}\\
& \mathbf{W}_c \succeq 0,\ \mathbf{W}_s \succeq 0. && \text{(14d)}
\end{aligned}$$

If solutions $\mathbf{W}_c^*$ and $\mathbf{W}_s^*$ are not rank-1, then we can utilize Gaussian randomization to get approximated values of $\mathbf{w}_c$ and $\mathbf{w}_s$.

B. RIS phase ($\mathbf{\Phi}$) optimization for fixed $\mathbf{w}_c$ and $\mathbf{w}_s$

Let $\boldsymbol{\phi} = [e^{j\theta_1}, \ldots, e^{j\theta_N}]^H$. Then

$$\mathbf{h}^H\mathbf{\Phi}\mathbf{G}\mathbf{w}_i = \boldsymbol{\phi}^H\text{diag}(\mathbf{h}^H)\mathbf{G}\mathbf{w}_i = \boldsymbol{\phi}^H\mathbf{a}_i, \tag{15}$$

and

$$\mathbf{g}^H\mathbf{\Phi}\mathbf{G}\mathbf{w}_i = \boldsymbol{\phi}^H\text{diag}(\mathbf{g}^H)\mathbf{G}\mathbf{w_i} = \boldsymbol{\phi}^H\mathbf{b_i}, \tag{16}$$

where $\mathbf{a}_i = \text{diag}(\mathbf{h}^H)\mathbf{G}\mathbf{w}_i$ and $\mathbf{b}_i = \text{diag}(\mathbf{g}^H)\mathbf{G}\mathbf{w}_i$ for $i \in \{c, s\}$. Therefore, the expressions of γ_u and γ_x in Eqs. (3) and (5) can be modified as

$$\gamma_u = \frac{|\boldsymbol{\phi}^H\mathbf{a}_c|^2 + |\alpha\mathbf{f}|^2|\boldsymbol{\phi}^H\mathbf{b}_c|^2}{|\boldsymbol{\phi}^H\mathbf{a}_s|^2 + |\alpha\mathbf{f}|^2|\boldsymbol{\phi}^H\mathbf{b}_s|^2 + \sigma_u^2}. \tag{17}$$

$$\gamma_x = \frac{|\alpha\mathbf{r}|^2|\boldsymbol{\phi}^H\mathbf{b}_s|^2}{\sigma_x^2}. \tag{18}$$

We can rewrite the optimization problem (P1) as

$$(\text{P5}):\max_{\boldsymbol{\phi}} \quad \log_2\left(1+\frac{|\boldsymbol{\phi}^H\mathbf{a}_c|^2+|\alpha\mathbf{f}|^2|\boldsymbol{\phi}^H\mathbf{b}_c|^2}{|\boldsymbol{\phi}^H\mathbf{a}_s|^2+|\alpha\mathbf{f}|^2|\boldsymbol{\phi}^H\mathbf{b}_s|^2+\sigma_u^2}\right) \tag{19a}$$

$$\text{subject to} \quad |\boldsymbol{\phi}^H\mathbf{b}_s|^2 \geq \frac{\gamma_{\text{th}}\sigma_x^2}{|\alpha\mathbf{r}|^2}, \tag{19b}$$

$$|\phi_m| = 1, \quad \forall m. \tag{19c}$$

Using Minorization-Maximization (MM) for the solution, the objective function in (P5) can be shown as

$$\max_{\boldsymbol{\phi}} \quad \frac{\boldsymbol{\phi}^H\mathbf{A}\boldsymbol{\phi}}{\boldsymbol{\phi}^H\mathbf{B}\boldsymbol{\phi}+\sigma_u^2}, \tag{20}$$

where $\mathbf{A}=\mathbf{a}_c\mathbf{a}_c^H+|\alpha\mathbf{f}|^2\mathbf{b}_c\mathbf{b}_c^H$, and $\mathbf{B}=\mathbf{a}_s\mathbf{a}_s^H+|\alpha\mathbf{f}|^2\mathbf{b}_s\mathbf{b}_s^H$. This problem still shows the non-convexity. Therefore, we employ a quadratic transform for fractional programming to express the fractional objective in (20) in a quadratic form as

$$\max_{\boldsymbol{\phi},y} \quad 2y\sqrt{\boldsymbol{\phi}^H\mathbf{A}\boldsymbol{\phi}}-y^2(\boldsymbol{\phi}^H\mathbf{B}\boldsymbol{\phi}+\sigma_u^2), \tag{21}$$

where y is a complex scalar auxiliary variable to linearize the fractional objective. We can alternate between optimizing y and $\boldsymbol{\phi}$. So $\boldsymbol{\phi}$ can be optimized by considering the fixed y to maximize the $2y\sqrt{\boldsymbol{\phi}^H\mathbf{A}\boldsymbol{\phi}}-y^2\boldsymbol{\phi}^H\mathbf{B}\boldsymbol{\phi}$. By using the first-order approximation via MM at point $\boldsymbol{\phi}_0$, we approximate

$$\sqrt{\boldsymbol{\phi}^H\mathbf{A}\boldsymbol{\phi}} \approx \frac{1}{2}\frac{\boldsymbol{\phi}_0^H\mathbf{A}\boldsymbol{\phi}_0}{\sqrt{\boldsymbol{\phi}_0^H\mathbf{A}\boldsymbol{\phi}_0}}+\frac{1}{2}\frac{\boldsymbol{\phi}^H\mathbf{A}\boldsymbol{\phi}_0}{\sqrt{\boldsymbol{\phi}_0^H\mathbf{A}\boldsymbol{\phi}_0}}, \tag{22}$$

then solving the following

$$(\text{P6}):\max_{\boldsymbol{\phi}} \quad y\frac{\boldsymbol{\phi}^H\mathbf{A}\boldsymbol{\phi}}{\sqrt{\boldsymbol{\phi}_0^H\mathbf{A}\boldsymbol{\phi}_0}}-y^2\boldsymbol{\phi}^H\mathbf{B}\boldsymbol{\phi} \tag{23a}$$

$$\text{subject to} \quad (19b), (19c). \tag{23b}$$

We use projected gradient descent to update the $\boldsymbol{\phi}$ as follow

$$\boldsymbol{\phi}^{t+1}=\boldsymbol{\phi}^t+\nabla f(\boldsymbol{\phi}^{(t)}) \tag{24}$$

where

$$\nabla f(\boldsymbol{\phi})=\frac{2A\boldsymbol{\phi}(\boldsymbol{\phi}^HB\boldsymbol{\phi}+\sigma_u^2)-2B\boldsymbol{\phi}(\boldsymbol{\phi}^HA\boldsymbol{\phi})}{(\boldsymbol{\phi}^HB\boldsymbol{\phi}+\sigma_u^2)^2}, \tag{25}$$

denotes the gradient of the objective function with respect to $\boldsymbol{\phi}$ and serves as the ascent direction in the projected-gradient update.

IV. Simulation Results

In this section, we provide the simulation results to show the performance of our proposed algorithm in terms of the user's communication rate for different numbers of RIS elements and sensing threshold values. For the the simulation setup we choose $M=8$, $N=32$, γ_{th} = 0 dB, P_{max} = 30 dBm, α = 1 and $\sigma_u^2=\sigma_x^2$ = 0 dBm.

Algorithm 1 Alternating Optimization for Joint Beamforming and RIS Phase Design

Input: Channel matrices h, g, G, noise powers σ_u^2, σ_x^2, power budget $P_{\max}$, sensing threshold γ_{th}, gradient ascent step size ρ.

Output: Optimized beamformers w_c^*, w_s^* and RIS phase vector $\boldsymbol{\phi}^*$.

Initialize active beamformers $\mathbf{w}_c^{(0)}, \mathbf{w}_s^{(0)}$, RIS phase vector $\boldsymbol{\phi}^{(0)}$ with $|\phi_n|=1$, set $t=0$, tolerance ε.
repeat
  (a) Active beamformer optimization:
  Compute equivalent channels and form R_c.
  Apply Dinkelbach's Transform: iteratively solve the SDP for W_c^*, W_s^* and update η until convergence.
  Find w_c, w_s using Gaussian randomization if W_c^* and W_s^* are not rank-1.
  (b) RIS phase optimization:
  Compute y based on the current $\boldsymbol{\phi}^{(t)}$.
  Update RIS phases via projected-gradient ascent: $\boldsymbol{\phi}^{(t+1)}=e^{j\angle(\boldsymbol{\phi}^{(t)}+\rho\nabla f(\boldsymbol{\phi}))}$.
  $t \leftarrow t+1$.
until $|R_u^{(t)}-R_u^{(t-1)}|<\varepsilon$
return $w_c^*, w_s^*, \boldsymbol{\phi}^*=\boldsymbol{\phi}^{(t)}$.

First, we present the relationship between communication rate and number of RIS elements in Fig. 2. It is evident from the results that for a fixed sensing threshold, communication rate increases with RIS containing a higher number of elements, because a larger number of RIS elements provides more spatial DoFs to enhance the communication performance of the RIS-assisted ISAC system. On the other hand, if we change the sensing threshold, the communication rate shows higher performance at a low sensing threshold, because to meet the given sensing threshold for sensing SNR, our proposed system allocates the power for sensing from the total transmit power budget, and the rest of the power for communication. So, at a lower sensing threshold, more power can be allocated for communication, and to meet a higher sensing threshold, power allocation for communication will decrease accordingly. Therefore, the communication rate increases from a higher to a lower sensing threshold. It gives us a trade-off between communication and sensing power allocation to achieve satisfactory communication and sensing performance of the ISAC system.

The communication rate versus sensing threshold for different numbers of RIS elements is shown in Fig. 3. Results show that the communication rate goes down by increasing the value of the sensing threshold for a fixed number of RIS elements. Nevertheless, the communication rate gives better performance as we fix the higher number of RIS elements.

We present a comparison of our proposed algorithm with random RIS and no RIS baseline schemes in Fig. 4. It is clear that our proposed algorithm with optimized RIS phase shift results in a higher communication rate with the increasing

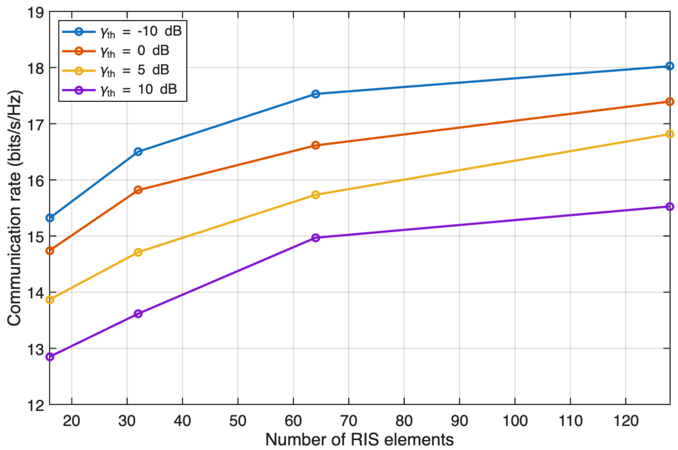

Figure 2. Communication versus number of RIS elements for different values of sensing threshold.

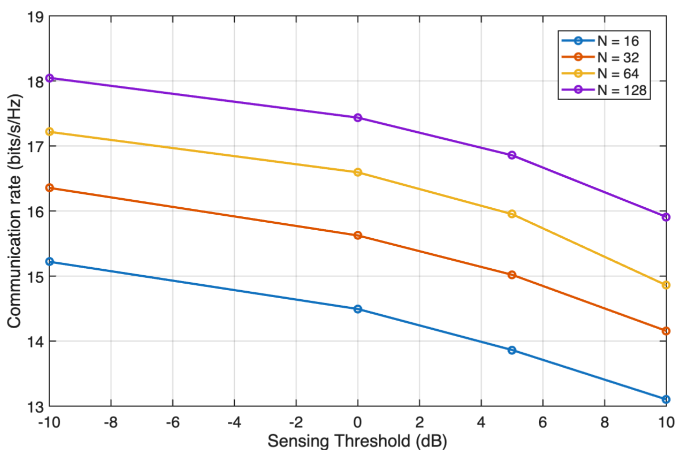

Figure 3. Communication rate versus sensing threshold for different number of RIS elements.

number of RIS elements at a fixed sensing threshold. In a random RIS case, we set RIS phase shift independently and uniformly at random over the interval $[0, 2\pi)$ without optimizing the RIS phases, which leaves the system fully dependent on random multipath conditions. Hence, random RIS provides us a lower bound of the system's performance, which can be improved by optimizing the RIS phase shift, and it is clear that our proposed algorithm shows better performance than this baseline scheme. In the case of no RIS, the communication rate lies on the x-axis because a direct link between the transmitter and the user is blocked. It means that without RIS, no communication can take place with the user in the given scenario.

Similarly, in Fig. 5, communication rate versus sensing threshold with a fixed number of RIS elements is compared with the above-mentioned two baseline schemes. Results show that our proposed algorithm outperforms by achieving a higher communication rate as compared to other baseline schemes. It is also to note that the communication rate decreases by increasing the sensing threshold.

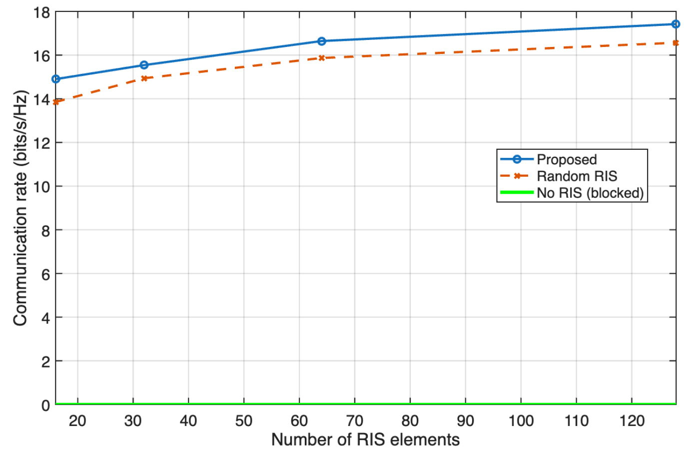

Figure 4. Comparison with other scheme for fixed value of sensing threshold.

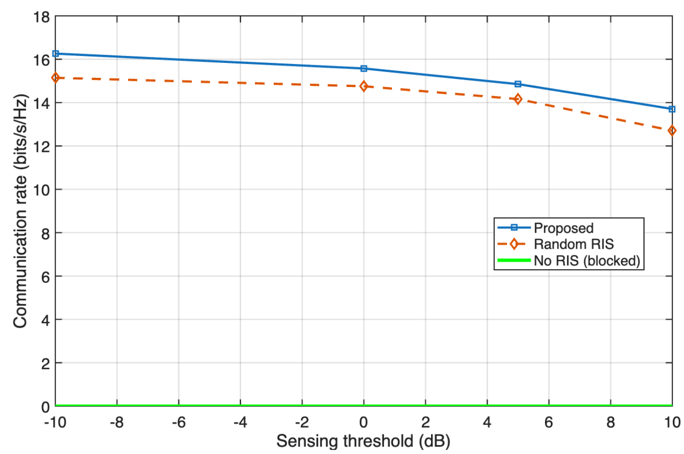

Figure 5. Comparison with other scheme for fixed number of RIS elements.

V. Conclusion

This paper investigates a RIS-assisted bi-static ISAC system with the assumption that both the user and target are located close to each other. The reflected sensing signal from the target received at the communication user can affect the user's communication rate. We aim to jointly optimize the transmit beamformer and the RIS reflection coefficients to maximize the user's communication rate while satisfying the minimum sensing SNR requirement, transmit power, and RIS unit-modulus constraints. To solve this non-convex problem, an efficient AO algorithm is developed by leveraging the FP, SDR, and MM techniques. Simulation results show that the proposed scheme gives better performance as compared to random RIS and no RIS schemes. Results show that the communication rate increases with increasing number of RIS elements and decreases when the sensing threshold increases. For our future direction, this work will be extended to a multi-user and multi-target scenario.

Acknowledgment

This work was supported by the National Research Foundation of Korea (NRF) grant funded by the Korea government

(MSIT) (No. RS-2024-00409492).

REFERENCES

[1] Y. Chen, Z. Ren, J. Xu, Y. Zeng, D. W. K. Ng, and S. Cui, "Integrated sensing, communication, and powering: Toward multi-functional 6G wireless networks," *IEEE Commun. Mag.*, vol. 63, no. 8, pp. 146–153, Aug. 2025.

[2] S. Aldirmaz-Colak, M. Namdar, A. Basgumus, S. Özyurt, S. Kulac, N. Calik, M. A. Yazici, A. Serbes, and L. Durak-Ata, "A comprehensive review on ISAC for 6G: Enabling technologies, security, and AI/ML perspectives," *IEEE Access*, 2025.

[3] F. Liu, Y. Cui, C. Masouros, J. Xu, T. X. Han, Y. C. Eldar, and S. Buzzi, "Integrated sensing and communications: Toward dual-functional wireless networks for 6G and beyond," *IEEE J. Sel. Areas Commun.*, vol. 40, no. 6, pp. 1728–1767, Jun. 2022.

[4] S. Lu, F. Liu, Y. Li, K. Zhang, H. Huang, J. Zou, X. Li, Y. Dong, F. Dong, J. Zhu, Y. Xiong, W. Yuan, Y. Cui, and L. Hanzo, "Integrated sensing and communications: Recent advances and ten open challenges," *IEEE Internet Things J.*, vol. 11, no. 11, pp. 19 094–19 120, Jun. 2024.

[5] Z. Wei, F. Liu, C. Masouros, N. Su, and A. P. Petropulu, "Toward multi-functional 6G wireless networks: Integrating sensing, communication, and security," *IEEE Commun. Mag.*, vol. 60, no. 4, pp. 65–71, Apr. 2022.

[6] C. Zeng and H. Li, "Beamforming optimization for RIS-assisted RF sensing in multipath NLOS environments," *IEEE Sensors Lett.*, vol. 9, no. 7, pp. 1–4, Jul. 2025.

[7] Z. Zhang, L. Dai, X. Chen, C. Liu, F. Yang, R. Schober, and H. V. Poor, "Active RIS vs. passive RIS: Which will prevail in 6G?" *IEEE Trans. Commun.*, vol. 71, no. 3, pp. 1707–1725, Mar. 2023.

[8] M. Ahmed, S. Raza, A. Amin Soofi, F. Khan, W. Ullah Khan, S. Zain Ul Abideen, F. Xu, and Z. Han, "Active reconfigurable intelligent surfaces: Expanding the frontiers of wireless communication-a survey," *IEEE Commun. Surveys Tuts.*, vol. 27, no. 2, pp. 839–869, Apr. 2025.

[9] B. Wang, C. Pan, H. Ren, Z. Yu, Y. Zhang, M. Liu, and G. Zhou, "Beamforming design for double-active-RIS-aided communication systems with inter-excitation," *IEEE Trans. Wireless Commun.*, vol. 24, no. 7, pp. 5855–5870, Jul. 2025.

[10] C. Pan, G. Zhou, K. Zhi, S. Hong, T. Wu, Y. Pan, H. Ren, M. D. Renzo, A. Lee Swindlehurst, R. Zhang, and A. Y. Zhang, "An overview of signal processing techniques for RIS/IRS-aided wireless systems," *IEEE J. Sel. Topics Signal Process.*, vol. 16, no. 5, pp. 883–917, Aug. 2022.

[11] J. Lou, C. Jiang, X. Han, and X. Wang, "A standardization framework for channel modeling in RIS-assisted integrated sensing and communication systems," *IEEE Commun. Stand. Mag.*, vol. 8, no. 4, pp. 48–53, Dec. 2024.

[12] D. An, J. Hu, and C. Huang, "Joint design of transmit waveform and passive beamforming for RIS-assisted ISAC system," *Signal Process.*, vol. 204, p. 108854, Mar. 2023.

[13] V. Kumar and M. Chafii, "Beamforming design for secure RIS-enabled ISAC: Passive RIS versus active RIS," *IEEE Trans. Wireless Commun.*, vol. 24, no. 9, pp. 7719–7732, Sep. 2025.

[14] M. Li, S. Zhang, Y. Ge, and C. Yuen, "STAR-RIS aided dynamic scatterers tracking for integrated sensing and communications," *IEEE Trans. Veh. Technol.*, vol. 74, no. 5, pp. 7760–7773, May. 2025.

[15] Z. Wu and W. Zhang, "Joint transmit and reflect beamforming design for active-RIS-assisted secure ISAC systems," *IEEE Wireless Commun. Lett.*, vol. 29, no. 8, pp. 1769–1773, Aug. 2025.

[16] L. Guo, J. Jia, X. Mu, Y. Liu, J. Chen, and X. Wang, "Joint secure and covert communications for active STAR-RIS assisted ISAC systems," *IEEE Trans. Wireless Commun.*, vol. 24, no. 9, pp. 7501–7516, Sep. 2025.

[17] F. Wang, N. Li, K. Yang, and X. Tao, "IRS-aided bi-static ISAC system with security constraint," in *Proc. 30th Annu. Int. Conf. Mobile Comput. Netw. (MobiCom)*, Washington D.C., DC, USA, Nov. 2024, pp. 2222–2229.